Power Source Characterization for Microgrid Systems

California Polytechnic State University, San Luis Obispo
Electrical Engineering Department

Senior Project Faculty Advisor: Dr. Poon

Authors: Jalius Welch, Chris Crossan

Spring 2023

Contents

List of Figures

List of Tables

Abstract

Our project aims to develop an affordable and versatile device for testing and analyzing solar panels, batteries, and other voltage sources. The primary objective is to create a portable, cost-effective, and space-efficient device that can be used in various scenarios, including the evaluation of remote microgrids and specialized systems. The device will enable users to gather crucial information about the voltage-current relationship, voltage-power relationship, and other power characteristics of each test source across a range of load currents.

One key aspect of the device is its configurability, allowing users to easily modify device parameters and components to accommodate different use cases. This includes supporting lower or higher power sources, adapting to sources with different characteristic curves, and accommodating a wide input source voltage range. By providing users with digestible and valuable data, the device will facilitate the characterization and design of diverse energy systems that utilize these energy sources.

Introduction

The focus of our project is to analyze and characterize low-power DC sources suitable for microgrids. These sources encompass a variety of devices such as DC power supplies, rechargeable and non-rechargeable batteries, solar panels, and rectified/DC generators. The characterization process involves subjecting these sources to variable loading conditions across a range of currents while simultaneously measuring their voltage and power characteristics. Our main goal is to gather comprehensive data from each source, enabling us to visually and mathematically characterize their behavior. This characterization will provide valuable insights into the performance of each source when supplying power to a system.

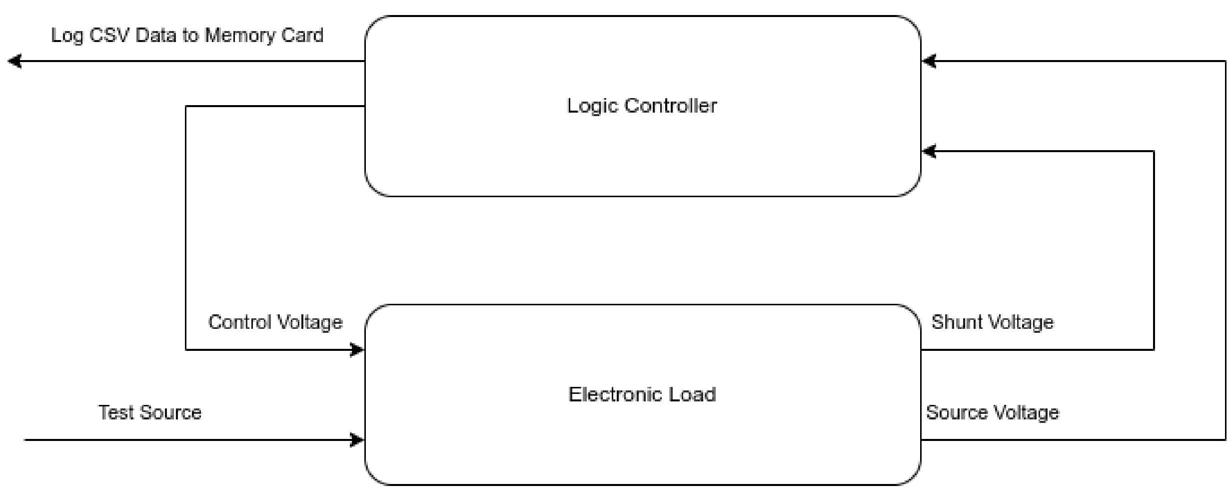

Figure 1. Power source characterization device top-level diagram.

Electronic Load Circuit Design

We start with a simple op amp control circuit that drives a power N-MOSFET, as shown in Fig. X. The circuit is effectively a V to I converter, that takes an input on the non-inverting terminal, and produces a matching output voltage (thus, setting output current) across the shunt resistor at the source side of the N-MOS by sensing via the inverting terminal.

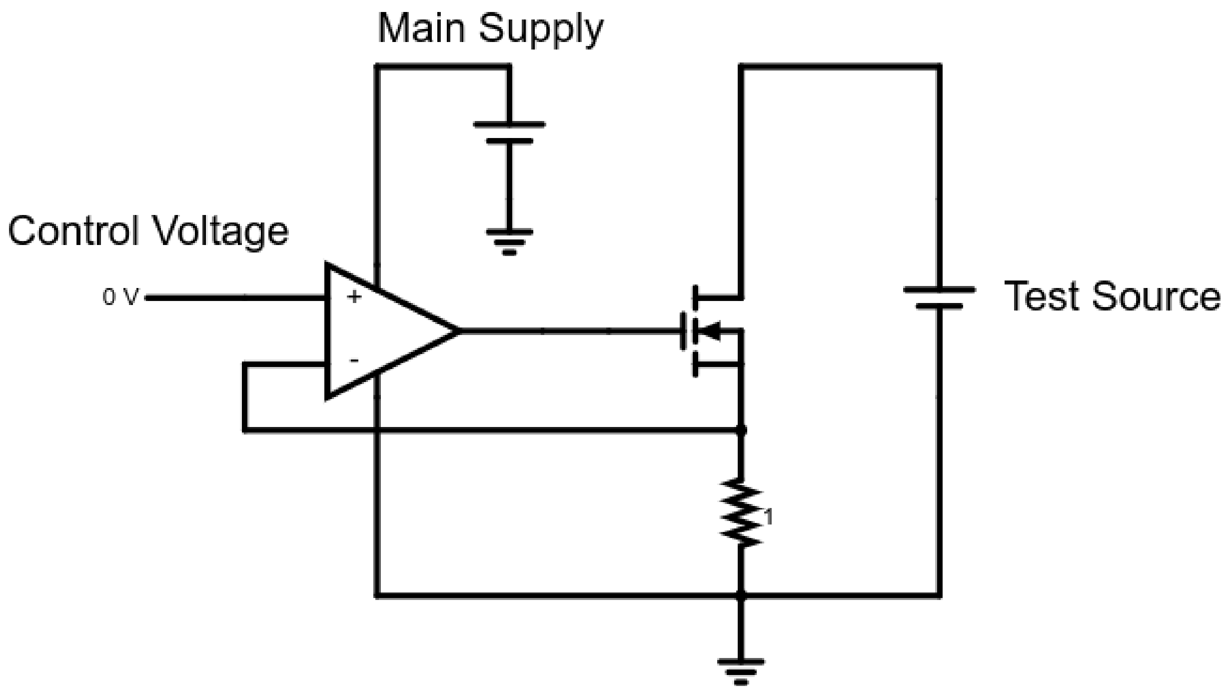

Figure 2. Low-fidelity representation of the electronic load circuit.

We chose an N-channel MOSFET to operate as a voltage controlled resistance for our load-side. The MOSFET should have low RDS on and should be able to operate in the ohmic region with non-linear VD to ID (RDS) behavior. Since the characteristics of MOSFETs do not have a linear VD to ID relationship, we should use active op amp control to allow for linear control of the MOSFET's RDS. The op amp's negative feedback will control the gate voltage in order to achieve nearly-linear VD to ID (RDS) behavior. Utilizing the MOSFET with a linear RDS, we can now specify component values, voltage, current, and power limits for the load-side.

Electronic Load - Limitations (Thermal, Power Dissipation)

When selecting components and determining heat sinking requirements for our electronic load, it is crucial to consider the limitations imposed by thermal factors and power dissipation. The main contributors to power consumption in the circuit are the MOSFET and shunt resistor. Since they are in series, they must be capable of dissipating the power from the test source. However, due to the dynamic nature of the power balance between the shunt and the MOSFET caused by the control circuitry, we need to consider two worst-case scenarios to determine the maximum power requirements for these components relative to the total allowable maximum power of the test source, $P_{TS\text{-}Max}$.

The first limiting case involves an ideal current source input, where the FET is fully on with low R_{DS} and the resistor dissipates almost all power from the test source. The second limiting case assumes an ideal voltage source input with high voltage, where R_{DS} is much higher than R_{Shunt} to maintain current, resulting in the majority of power being dissipated by the FET. Considering the dynamic power dissipation in the circuit, it is advisable to choose the FET and shunt resistor with nearly equal power dissipation capabilities. Finally, the maximum power dissipation of the electronic load circuit will be the minimum of the individual power dissipation capabilities of the FET and the shunt.

To ensure the safety of the devices and users, it is important to set an upper limit for the device temperature. We choose 70°C as our maximum temperature to mitigate the risk of burns [3]. Now, we must work backwards to determine the maximum power and heat-sinking requirements for the FET to maintain this temperature. Given the thermal resistance of the FET in the TO-220 package (approximately 70°C/W), it is clear that we need to include a heatsink if we want to increase the power capabilities of the circuit, which is desirable because it will increase the range of sources that we can test.

We can first calculate the baseline thermal behavior of the FET without a heatsink and determine thermal resistance equations for the behavior of the device's temperature as a function of power dissipation. With no heatsink, the total thermal resistance of the device (given in °C/W) is equal to the thermal resistance between the internal silicon and the base of the package plus the thermal resistance between the base of the package and the ambient air.

$$R_{TH(TOT)} = R_{TH(J-MB)} + R_{TH(MB-A)} = 1.5\,°C/W + 70\,°C/W = 71.5\,°C/W$$

By rearranging the equation, we can determine the maximum power as a function of the FET's thermal resistance and the desired maximum temperature.

$$T_{max} = T_{amb} + R_{TH(TOT)} * P_{max}$$

$$P_{max} = \frac{T_{max} - T_{amb}}{R_{TH(TOT)}}$$

We can compute the maximum FET power at the low-end of 25°C and high-end of 50°C ambient temperatures to be less than 1W. Clearly, it would be beneficial to add a heatsink.

Now we have an equation governing the maximum FET power as a function of temperatures and heatsink thermal resistance, which will allow us to select a heatsink based on the parameters.

$$P_{max} = \frac{T_{max} - T_{amb}}{R_{TH(J-MB)} + R_{TH(MB-A)}}$$

Let's select a heatsink with $R_{TH(MB-A)}$ = 18.5°C/W and compute the maximum FET power.

$$P_{max} = \frac{70 - 25}{20} = 2.25W$$

$$P_{max} = \frac{70 - 50}{20} = 1W$$

Controller Selection

Considering the requirements for our project, we have made the decision to replace the Programmable Logic Controller (PLC) with a microcontroller. We chose to substitute a microcontroller for the PLC because it has lower cost, smaller size, and less energy consumption. The downsides are that the microcontroller is less tuned for industrial reliability and has less support and development software. The tradeoff is acceptable for the scope of this project, and we can always rewrite the software on the PLC to utilize an identical measurement circuit.

Our device requires a microcontroller with ADC and DAC in order to output and sample the signals required for energy source characterization. Furthermore, it is essential to choose a microcontroller that supports the required communication protocols for interfacing with other components and external devices. This includes protocols such as UART and SPI for transmitting data to a connected computer and to the SD card reader.

Controller Logic and Function

The microcontroller software serves to test and record the characteristics of the test source attached to the electronic load. The microcontroller will control the current through the load using the measurement circuitry inputs. The microcontroller will record current, voltage, and power at multiple points to create an I-V plot and max power characteristics plot. The microcontroller will monitor fault conditions of the measurement circuitry during operation, such as overcurrent, overvoltage, and overpower and pause testing if faults are detected.

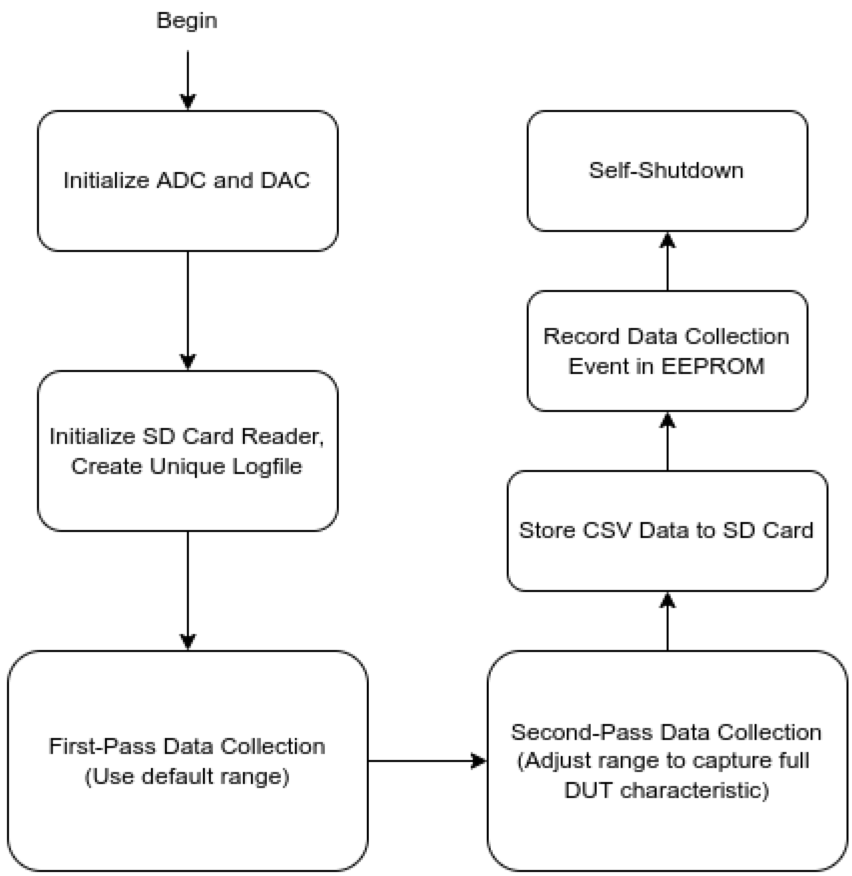

Figure 3. Data collection and recording program flowchart.

Controller Resolution and Limitations

The microcontroller's ADC is 10 bits, and the DAC is 8 bits. From this and the reference voltage, we can compute the resolution of the voltage readings and outputs.

$$\frac{V_{ref}}{2^{ADC_{RES}}} = \frac{5}{2^{10}} = 4.88mV \qquad \frac{V_{ref}}{2^{DAC_{RES}}} = \frac{5}{2^{8}} = 19.53mV$$

Taking the nominal 5V supply as the reference, the ADC has ~5mV resolution and the DAC has ~20mV resolution. The low DAC resolution limits the amount of samples that we will be able to take with the measurement circuitry. The DAC controls the input side of the electronic load control circuitry. Since this corresponds to the output source current (1mV/mA == 1 Ω of R_{Shunt}), we would be limited to 10 samples from if we wanted to characterize the range 0 to 200mV (0 to 200mA on the output).

We would like a higher DAC resolution for the ability to take more data points from our source, especially if it's a low power source. To utilize a higher resolution in the DAC, we can use a resistive divider so that the DAC can operate over a wider range of voltages. This will effectively limit the DAC's range while increasing the resolution across the range. If we divide the DAC voltage by 10, we can thus take 100 measurements between 0 and 2000mV, which will accordingly span 0 to 200mA on the output.

We chose to divide the DAC voltage by 4.3 in order to provide approximately 4.54mV resolution on the DAC. This increase in the DAC resolution is important in ensuring accuracy when controlling the electronic load. The electronic load uses the DAC to control the input and the ADC to sample the output, and the relationship between input and output was configured to be 1:1 (from 1mV/mA == 1 Ω of R_{Shunt}). We record $I_{Test\text{-}Source}$ resolution as 4.54mA, which is derived from the DAC's 4.54mV resolution on the input side of the electronic load.

It is important that the ADC resolution is less than or equal to the DAC resolution, to preserve data accuracy through the electronic load. We considered using a different reference voltage in order to increase the dynamic range of the ADC. Instead, we decided to experiment with multiplying the output of the electronic load, which should ideally increase the accuracy of the ADC while decreasing its range. We chose to use the second channel of the LM358 op amp to multiply the shunt's output voltage by a factor of 6. In the absence of noise, this should increase the resolution of the $I_{Test\text{-}Source}$ measurements to 0.81mV. This will help increase our measurement accuracy, especially at the upper ranges of a test when the source current is tapering off. However, because $I_{Test\text{-}Source}$ is driven by a 4.54mV resolution input, we maintain this as its minimum resolution.

Table 1. Device data collection capabilities: resolution and ranges.

Parameter	**Resolution**	**Minimum**	**Maximum**	**Unit**
$N_{Data\text{-}Points}$	1	1	256	/
$I_{Test\text{-}Source}$	4.54	0	833.33	mA
$V_{Test\text{-}Source}$	10	0	$10 * 10^3$	mV

Aside from resolution, the DAC uses PWM which requires a low-pass filtering. For this we use a passive RC low-pass filter to attenuate the 490 Hz PWM signal. We must compensate for the attention to the PWM signal in software using a coefficient.

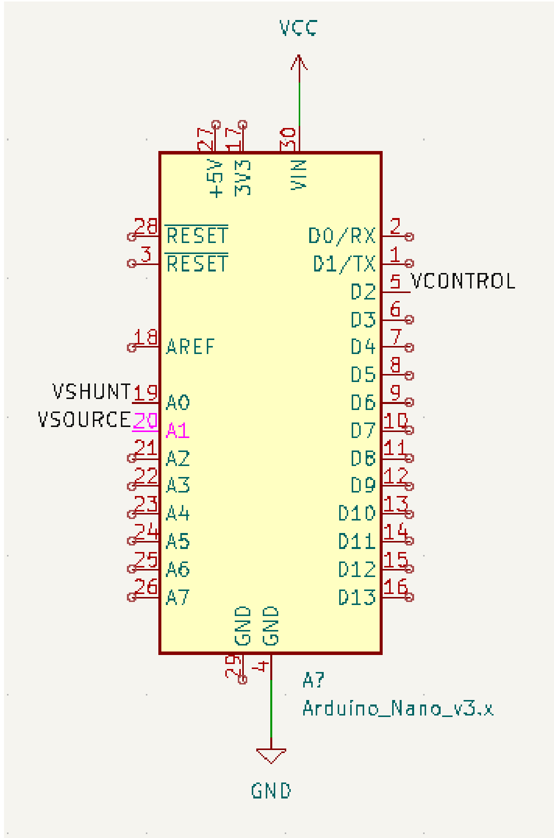

Figure 4. Microcontroller inputs and outputs - circuit diagram.

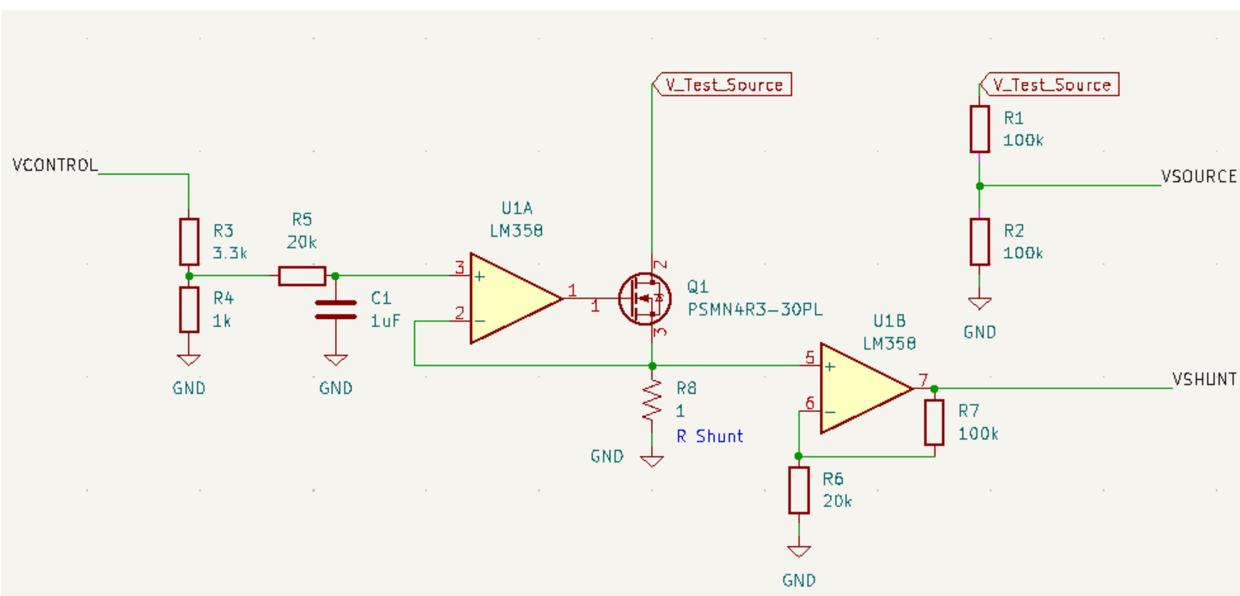

Figure 5. Electronic load and control circuitry diagram.

Device Characteristics and Ratings

Now that we have analyzed the circuit's power consumption, supply requirements, and microcontroller input and output limitations, we can determine the maximum ratings that characterize the device.

We shall set a maximum on the test source voltage by considering the limiting conditions. Firstly, we need to ensure the ADC on the microcontroller can read the source voltage without exceeding its range. The ADC range is 0V to 5V, which we extended to 0V to 10V through a ½ voltage divider. Secondly, we need to ensure the electronic load voltage limits are not exceeded, which can be determined from the DC safe operating area of the FET. Given our MOSFET's safe operating area, we can see that the DC safe operating area allows operation up to 30V at 1A. We should ensure the test source current and voltage do not exceed this value. The strictest of the test source voltage maximums comes from the microcontroller ADC. Therefore, the maximum test source voltage will be derived from the microcontroller's ADC maximum voltage, set at 10V.

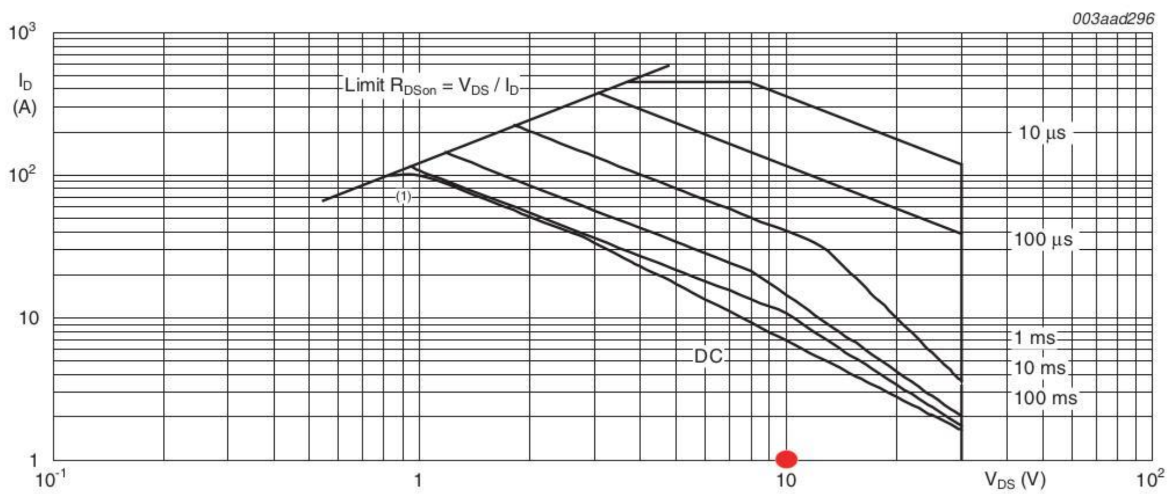

Figure 6. Safe operating area for the PSMN4R3 NMOS
(red dot shows selected operating point) [2].

Next we can set a maximum test source current and power. The main limiting conditions are: (1) safe operating area of the FET in DC, (2) the thermal limitations of the resistor and the FET, and (3) ADC for reading shunt voltage. We determined earlier that the safe operating area constrains the DC current of the FET to 1A with a maximum of 30 W. The power limitations of the FET come from the heat-sinking, and were calculated to be 2W as configured. The resistor is rated at 10W. The ADC that reads the shunt voltage was configured to have a range between 0 and 0.833V, for improved precision. This means that the maximum current that can be measured across the 1 Ω Resistor is 0.833A. The strictest power limit comes from the FET and the strictest current limit comes from the microcontroller's ADC. Therefore, we will set the maximum test source power to 2W and maximum test source current to 0.8A (maintaining the maximum source power limitation).

The supply voltage powers the op amp and feeds the microcontroller's voltage regulator. The maximum positive to negative supply voltage of the op amp is 36V. The voltage regulator that powers the microcontroller has a maximum voltage of 12V. The supply voltage maximum is set at 10V.

Table 2. Device maximum test source and supply ratings.

Parameter	**Conditions**	**Maximum**
Test Source Voltage	For any $I_{Test\text{-}Source}$	$V_{TS\text{-}Max}$ = 10 V
Test Source Current	$P_{TS} <= P_{TS\text{-}Max}$	$I_{TS\text{-}Max}$ = 0.8 A
Test Source Power	T_{amb} = 25°C, $R_{FET\text{-}Heatsink}$ = 18.5°C/W	$P_{TS\text{-}Max}$= 2 W
Supply Voltage	Limited by Microcontroller Regulator	$V_{S\text{-}Max}$ = 10 V

Table 3. Component selection, packages, and ratings.

Component	**Part Name**	**Package**	**Ratings**
R_{Shunt}	1 Ω Resistor	Axial	P_{max} = 10 W
N-MOSFET	PSMN4R3-30PL	TO-220	$V_{DS\text{-}Max}$ = 30V, $R_{DS(on)}$ = 4.3mΩ, P_{tot} = 103W @ T_{mb} = 25 °C
Dual op amp	LM358B	DIP-8	$V_{S\text{-}Max}$ = 36V
Microcontroller	ATMega328 / Nano	QFP64 / Prototype Board	$V_{S\text{-}Max}$ = 12V
$R_{Control}$	⅛ W Resistors	Axial	P_{max} = ⅛ W
Heatsink	TO-220 Heatsink	15*10*5 mm^3 bulk	$R_{TH\ (MB\text{-}A)}$ = 18.5 °C/W

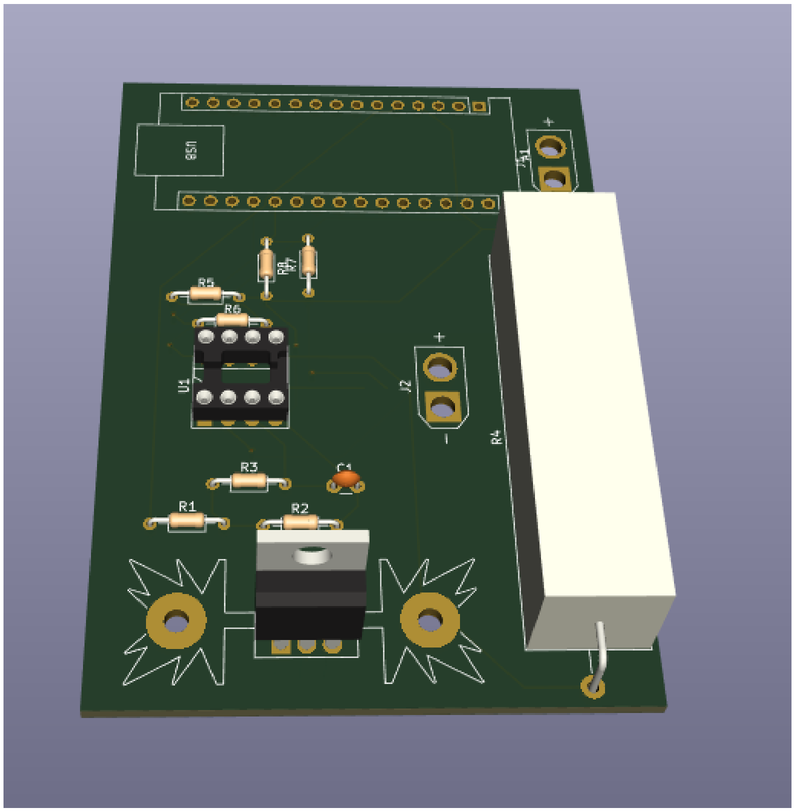

Figure 7. Rendering of the device on a commercially manufactured PCB.

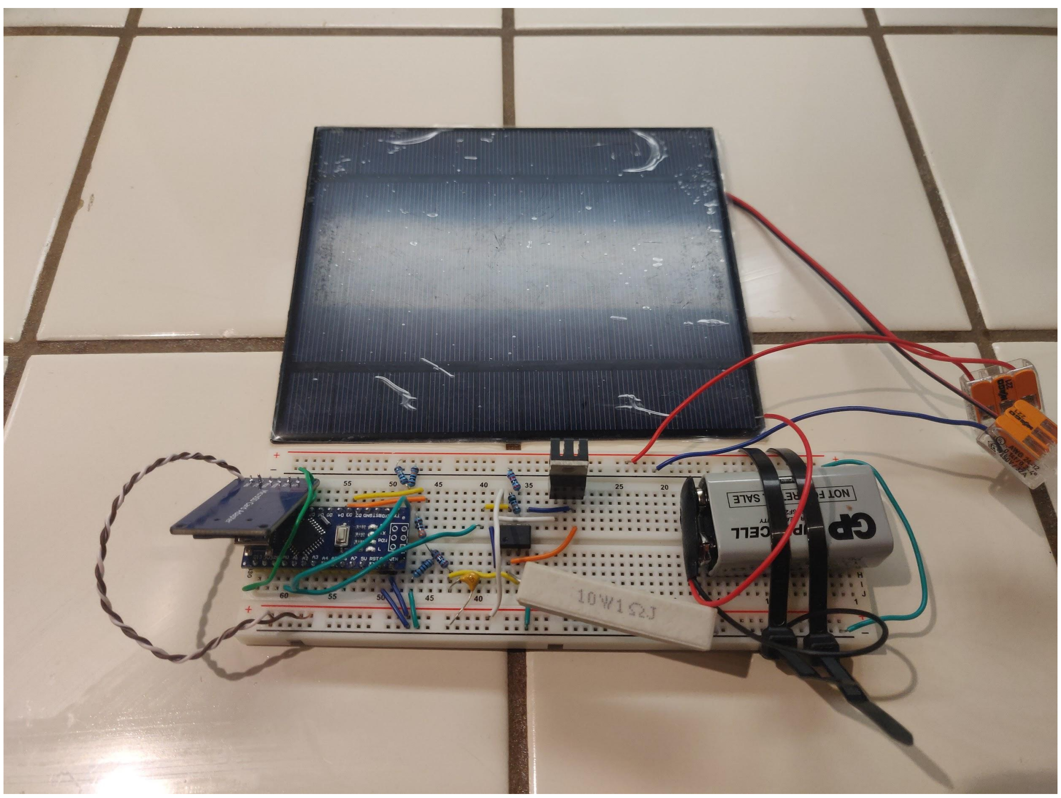

Figure 8. Breadboard device test setup.

Device Implementation, Operation, and Testing

The device was constructed on a breadboard with the components and characteristics as designed. The source characterization functionality of the device was tested using 3 photovoltaic test sources. On a day with minimal cloud cover at around 3:30PM, 3 solar panels of various sizes and characteristics were used to test the system and record data.

Table 4. Photovoltaic configuration used for initial device testing and data collection.

Test Source	Size	P_{RATED}	I_{SC} (A)	V_{OC} (V)
Small PV Panel	30 x 53 mm^2	0.25 W	0.024	5.7
Medium PV Panel	40 x 90 mm^2	100mA @ 7V = 0.7 W	0.112	9.0
Large PV Panel	150 x 130 mm^2	500mA @ 5V = 2.5W	0.545	6.1

A 9V battery was used as the supply voltage for the device, and the data collection was performed back-to-back for the 3 test sources.

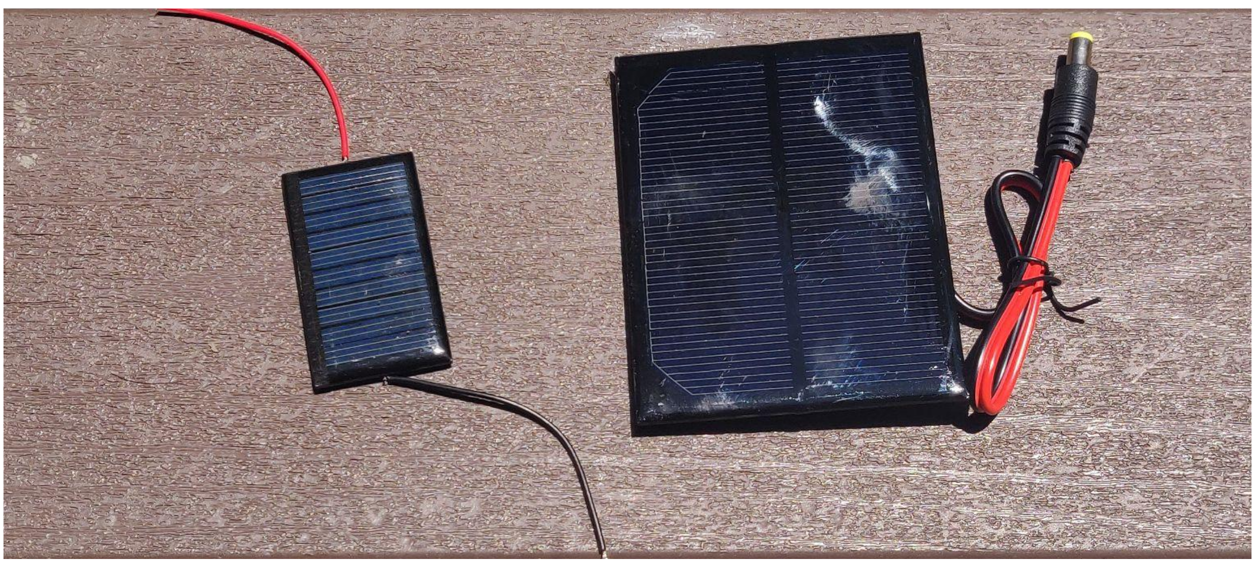

Figure 9. Small (left) and Medium (right) photovoltaic panels in test environment.

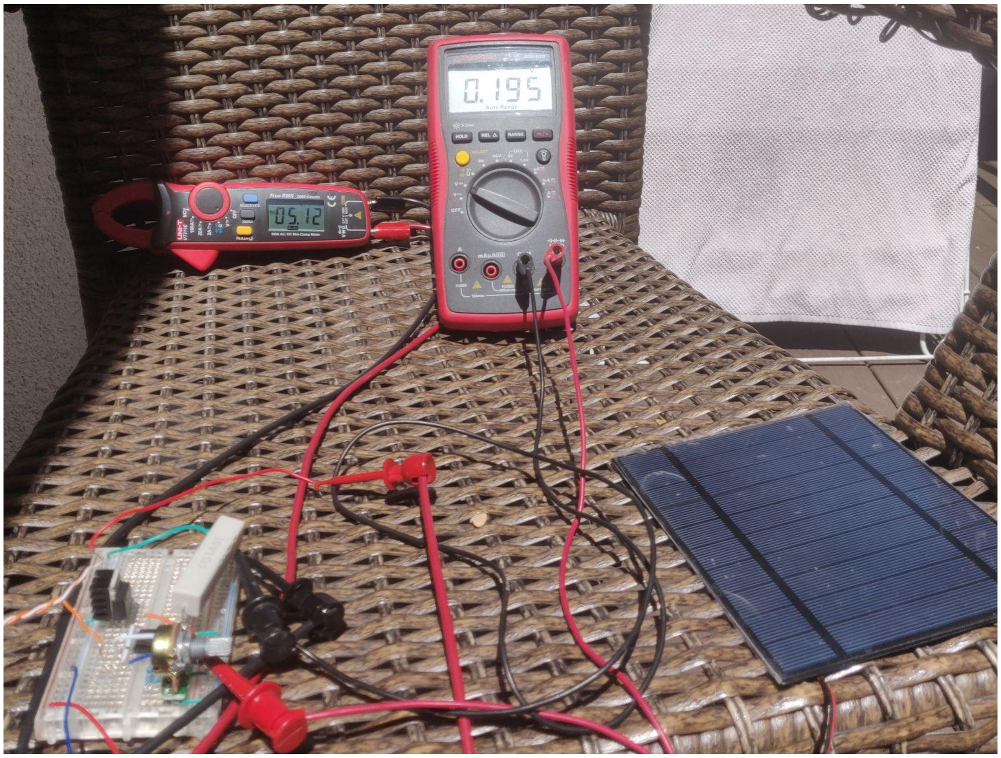

Figure 10. Large photovoltaic panel in test environment.

Data Observations

As observed in the data plots (Appendix A, Figs. 1-12), the panels all fall below their rated specifications for power. This can be attributed to the fact that the tests were run in the afternoon, after the period of maximum sun intensity which occurs around noon. The plots show that the device is accurately characterizing the source current to voltage and power to voltage relationships. The data collected is tabulated in Table 5, which compares the rated and observed power source behavior of the 3 tested photovoltaic panels.

Table 5. Test results and true characterization of the 3 photovoltaic panels.

Test Source	P_{RATED}	Measured Max Power	Deviation
Small PV Panel	0.25 W	21mA @ 5.425 V = 0.11W	-56%
Medium PV Panel	100mA @ 7V = 0.7W	84mA @ 7.263V = 0.61W	-12.9%
Large PV Panel	500mA @ 5V = 2.5W	250mA @ 4.858V = 1.21W	-51.6%

Observing the data for the small and medium panels (Appendix A, Figs. 5-12), there are certain gaps in the measurements with respect to source voltage. The gaps in the data are caused by the limited resolution of the DAC which drives the electronic load. The DAC is only capable of

4.54mV increments to the control circuitry, which in the small and medium panels led to gaps in the I/V, P/V, and general data plots. This is due to the fact that the data curves of the smaller sources fall into a smaller range of currents, which we were unable to measure using our relatively low resolution control system.

Reflection

Using a DAC with a better resolution, we would be able to drive the electronic load with a narrower current increment, and therefore collect data from the sources in narrower increments, and eliminate the gaps in the data. In addition to increasing the DAC resolution, we would also have to increase the ADC resolution, because as discussed earlier, the ADC resolution should be better or equal to the DAC resolution due to its role in the control circuitry on the output side of the electronic load. Additionally, in order to produce an appropriate amount of data points over the entire range, the control step (i.e. electronic load current) could be dynamically altered to collect evenly spaced data w.r.t. source voltage.

While a PLC was not used in the project as initially planned, a functional alternative was discovered and implemented in the form of a microcontroller. If further safety and reliability features are required, the microcontroller can be replaced by the PLC while maintaining the core functionality of the electronic load. Additionally, to improve on the design, a PCB and enclosure should be created to improve reliability and portability and to reduce board footprint.

Conclusion

In conclusion, the device functions as intended, and was able to capture data points to plot the IV characteristics of multiple test sources. The device can be used outdoors and off-grid with a battery source, which satisfies the portability requirement. The final device is low cost and low part count, making it easy to manufacture and distribute. While the device is capable of measuring a wide range of sources, the precision of the device suffers when testing low power sources. A solution is proposed to this problem, which involves increasing the DAC and ADC resolutions. Additionally, while the device is incapable of measuring higher-power sources, an increase to the heat-sinking is demonstrated to be feasible for increasing the power limit of the device. Overall, the device is functional, low cost, portable, and is useful in characterizing solar and other energy sources.

References

[1] “LM358,” *Ti.com*, 2022. https://www.ti.com/product/LM358 (accessed May 26, 2023).

[2] “PSMN4R3-30PL - N-channel 30 V 4.3 mΩ logic level MOSFET,” *Nexperia*. www.nexperia.com/products/mosfets/power-mosfets/PSMN4R3-30PL.html (accessed May 26, 2023).

[3] “Standard Guide for Heated System Surface Conditions that Produce Contact Burn Injuries,” *www.astm.org*. https://www.astm.org/c1055-20.html (accessed May 26, 2023).

[4] I. Hellman-Wylie and J. Navarro, “Microgrid Protection Student Laboratory,” *Cal Poly Electrical Engineering Senior Projects*, Jun. 2017, Accessed: May 26, 2023. [Online]. Available: https://digitalcommons.calpoly.edu/eesp/376

[5] N. Martinez, “Microgrid Protection Student Laboratory: Human-Machine Interface and SCADA Database,” *Cal Poly Electrical Engineering Senior Projects*, Jun. 2018, Accessed: May. 26, 2023. [Online]. Available: https://digitalcommons.calpoly.edu/eesp/433/

[6] S. M. Sharkh, M. A. Abu-Sara, G. I. Orfanoudakis, and B. Hussain, *Power Electronic Converters for Microgrids*. John Wiley & Sons, 2014.

[7] “Microgrids,” *www.nrel.gov*. https://www.nrel.gov/grid/microgrids.html (accessed May 26, 2023).

Appendix A - Data:

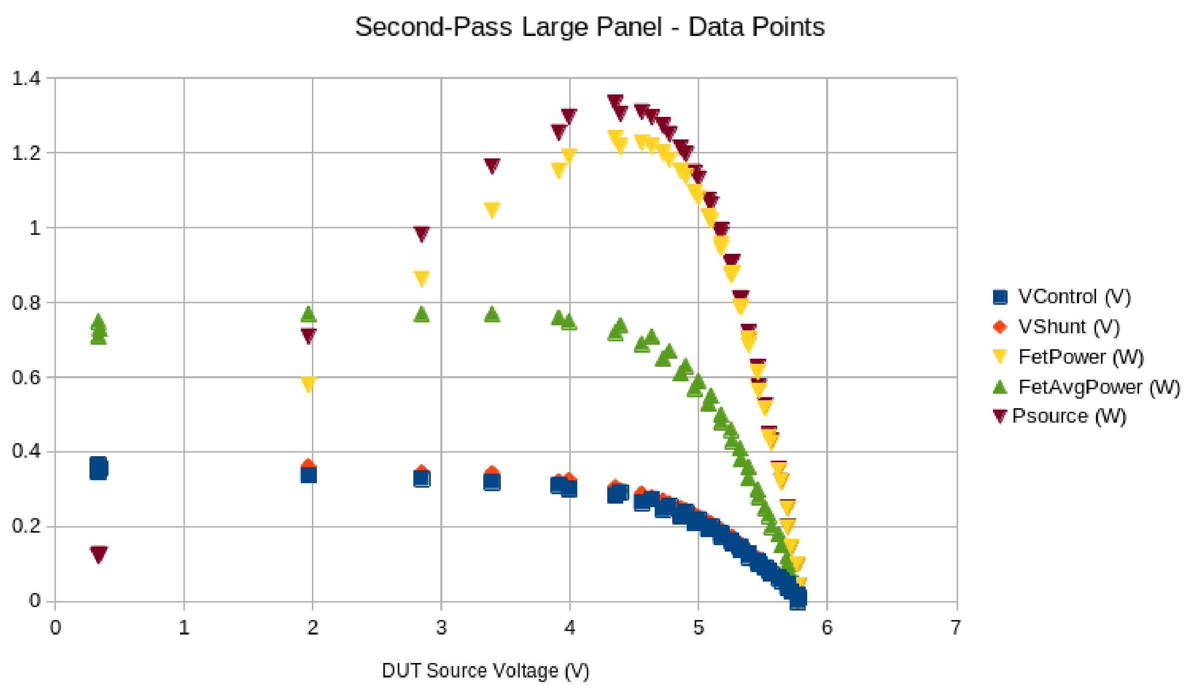

Figure 1A. Large panel load test: full data log plot.

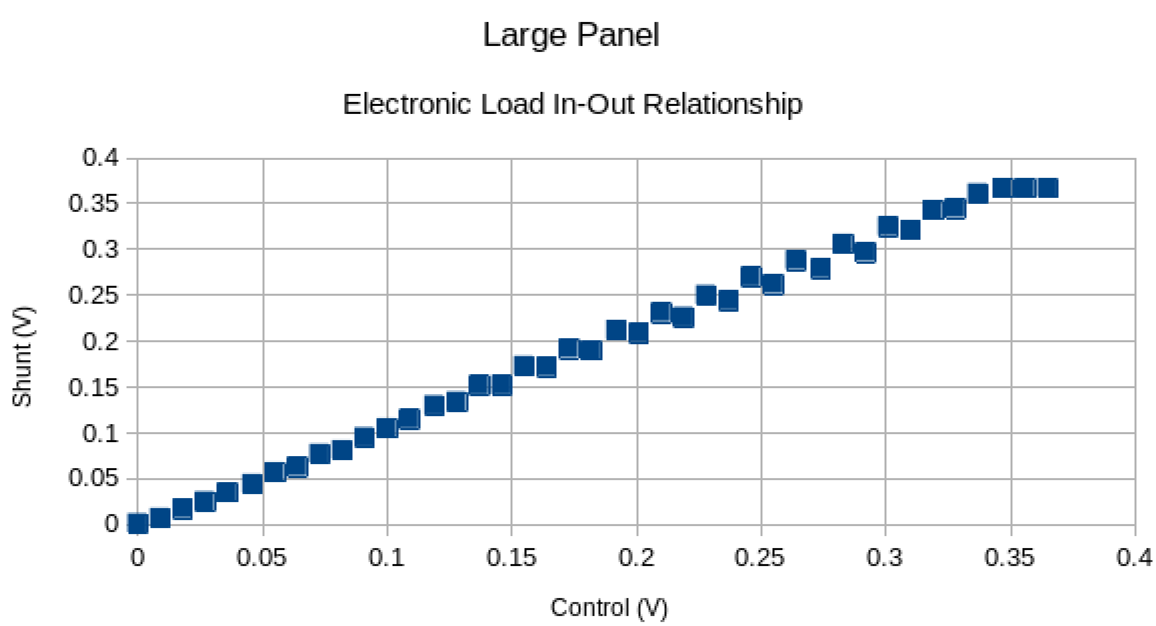

Figure 2A. Large panel load input/output relationship.

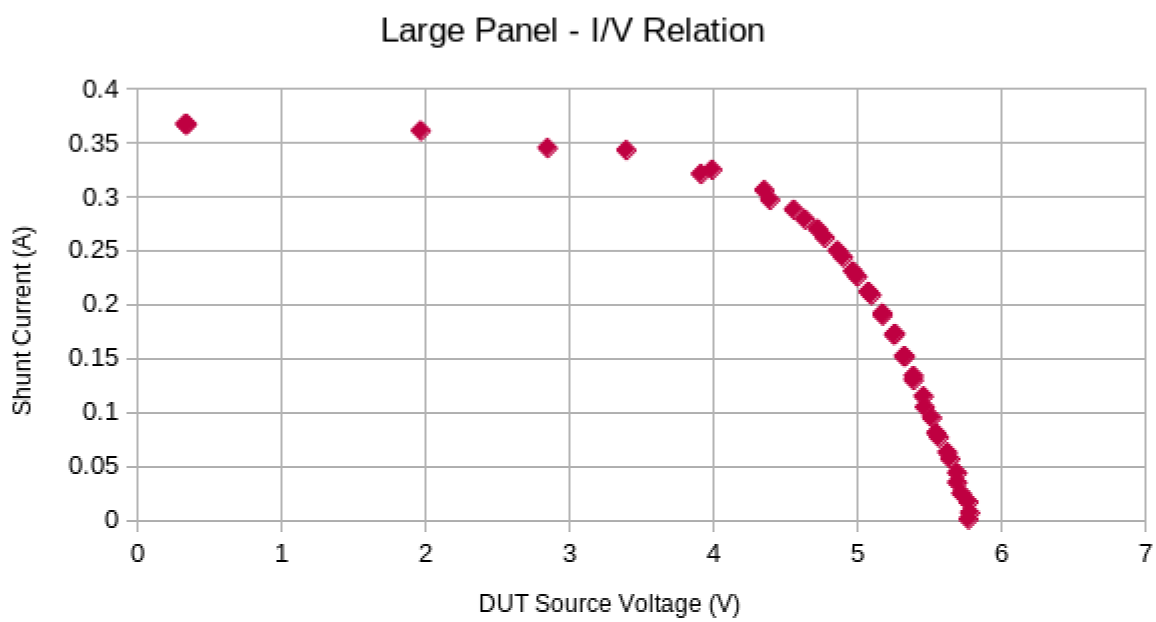

Figure 3A. Large panel load test: I/V relationship.

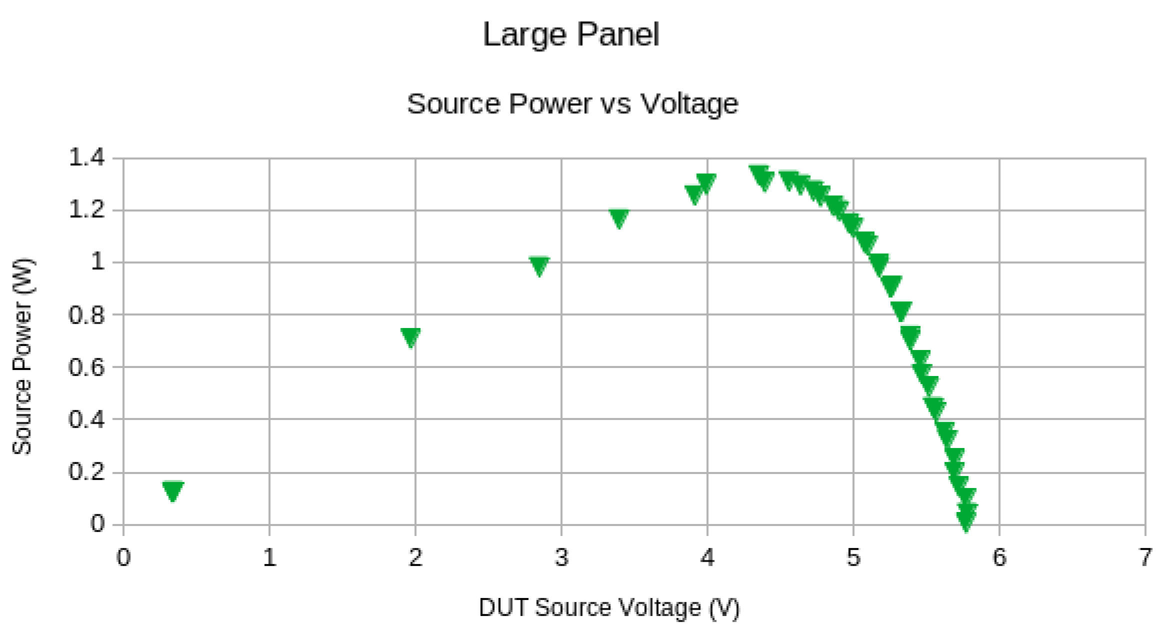

Figure 4A. Large panel load test: test source power vs voltage relationship.

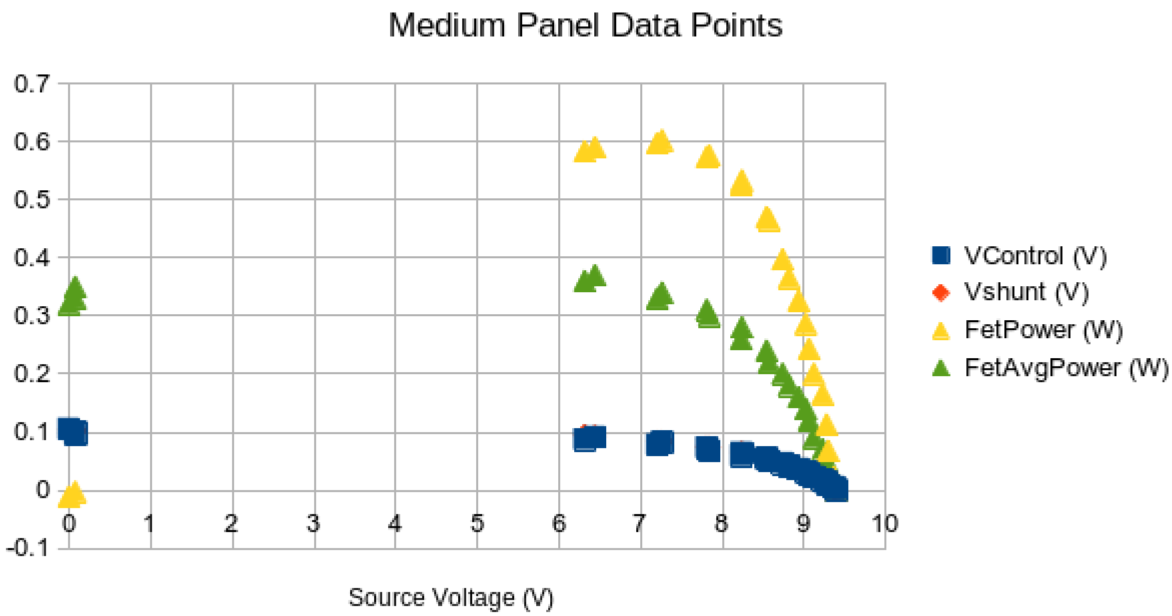

Figure 5A. Medium panel load test: full data log plot.

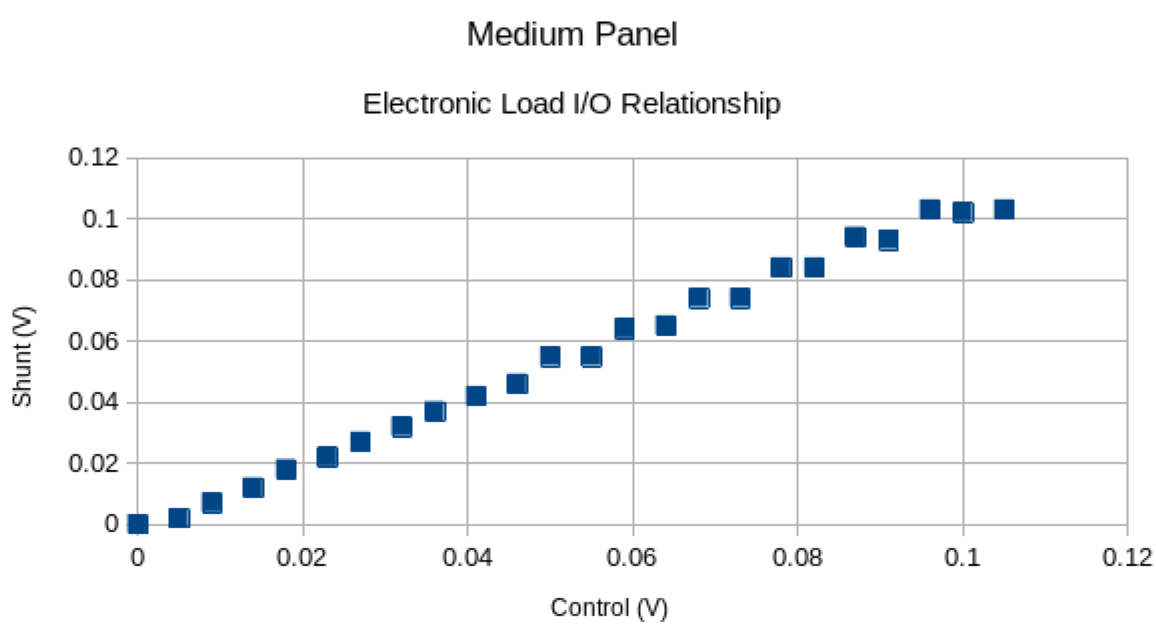

Figure 6A. Medium panel load input/output relationship.

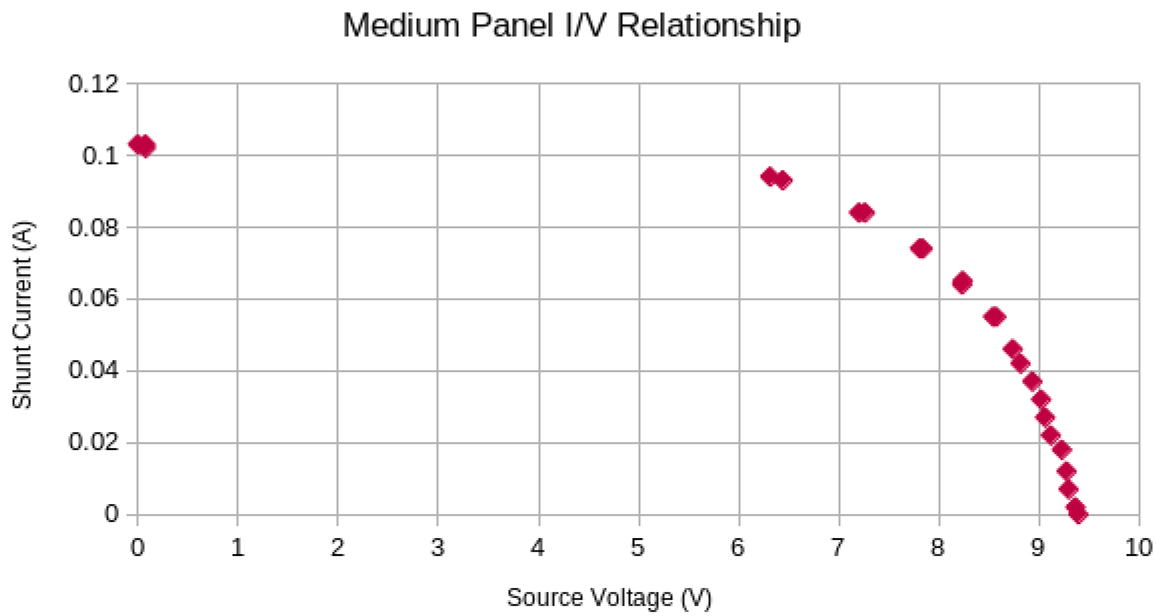

Figure 7A. Medium panel load test: I/V relationship.

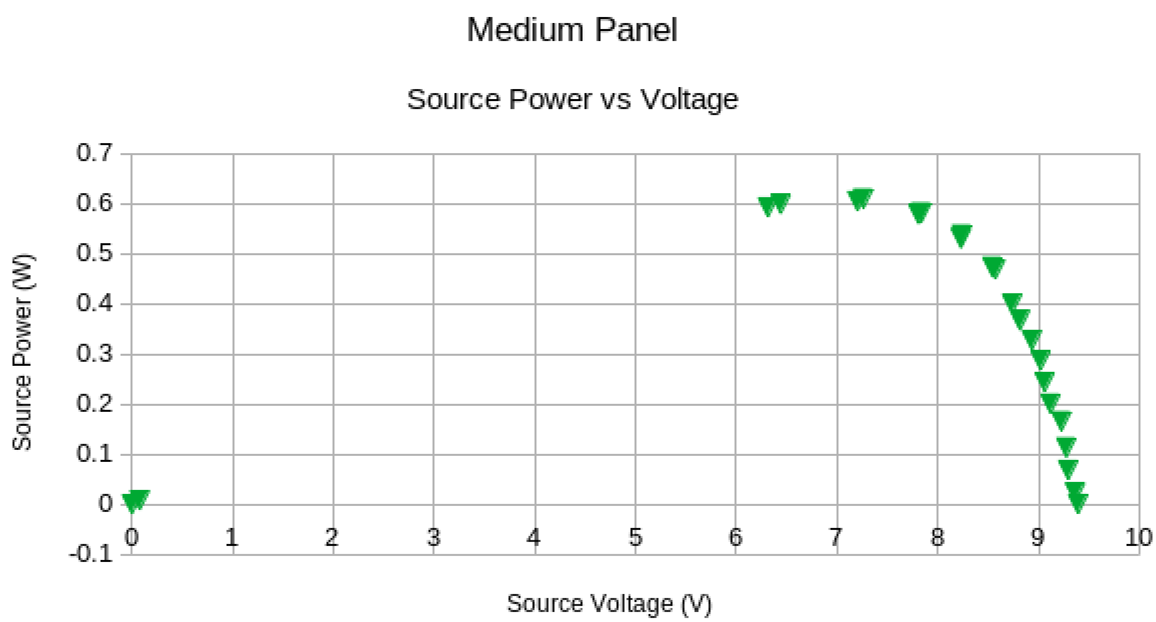

Figure 8A. Medium panel load test: test source power vs voltage relationship.

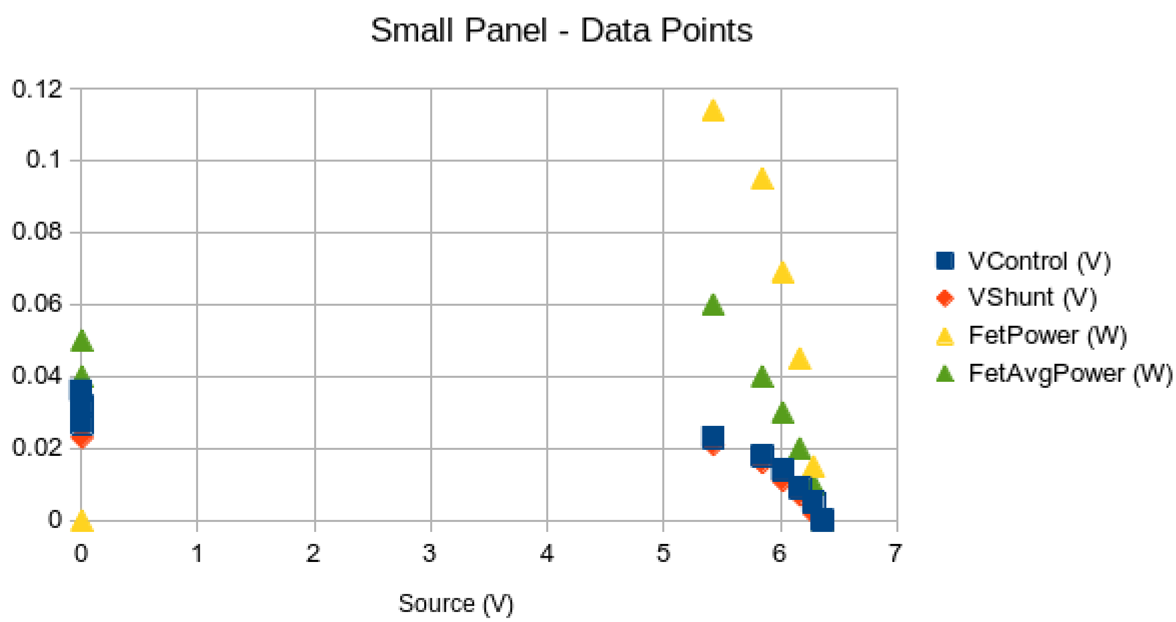

Figure 9A. Small panel load test: full data log plot.

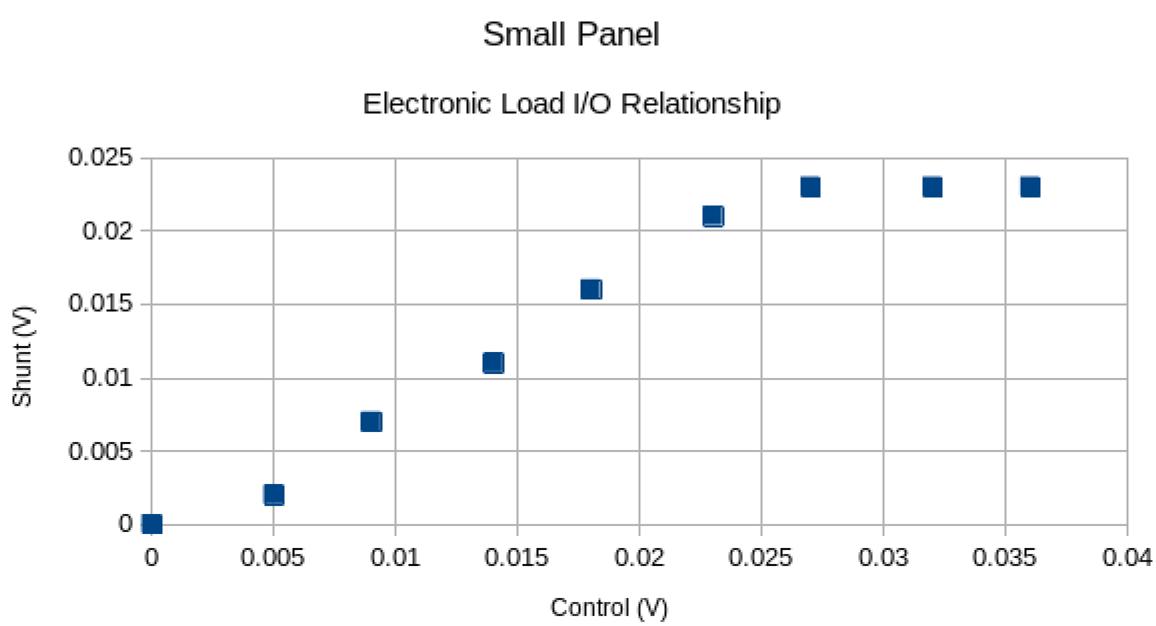

Figure 10A. Small panel load input/output relationship.

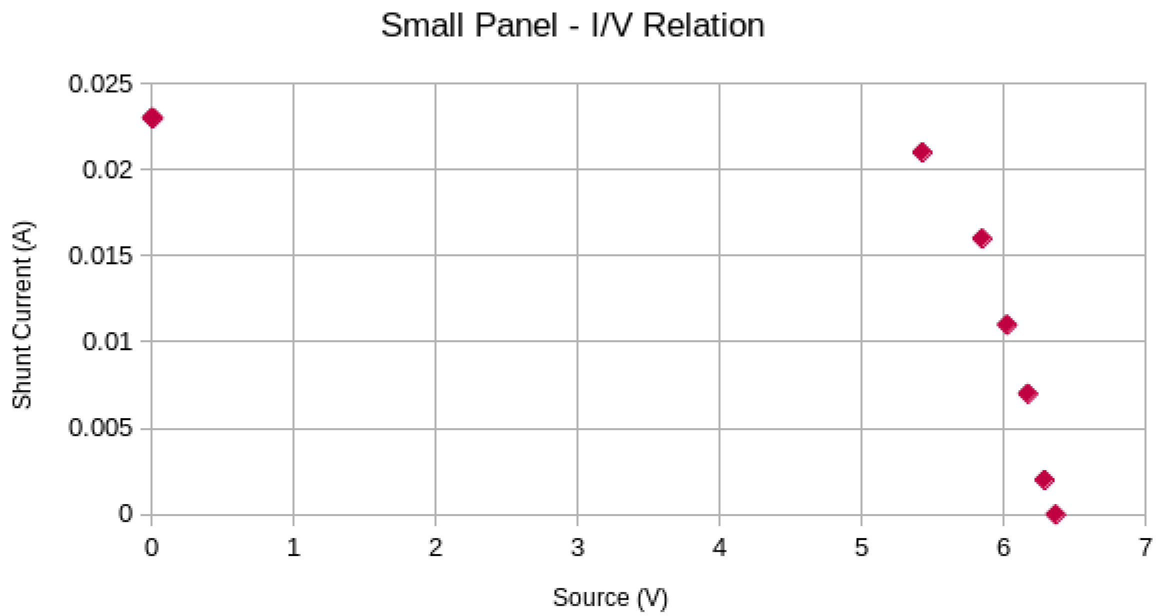

Figure 11A. Small panel load test: I/V relationship.

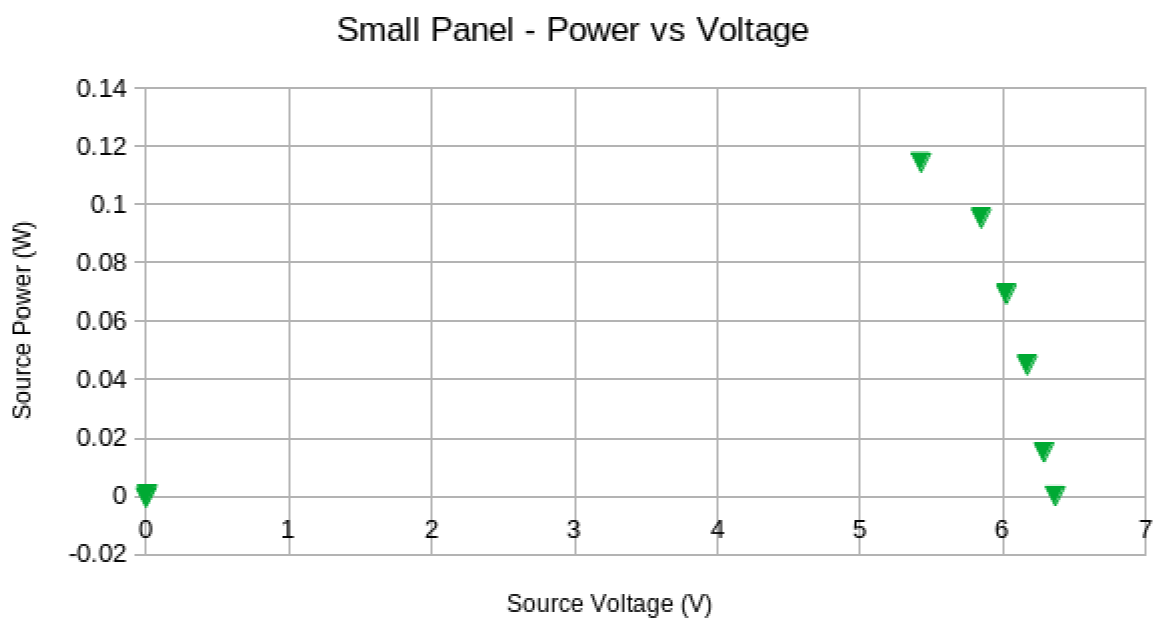

Figure 12A. Small panel load test: test source power vs voltage relationship.

Appendix B - Code:

```
#include <Arduino.h>
#include <SPI.h>
#include <SD.h>
#include <EEPROM.h>

constexpr int CHIP_SELECT = 9;

constexpr int FILENAME_CNT_EEPROM_ADR = 0;

//control network circuit constants
constexpr float v_source_divider_ratio = 2;
constexpr float v_control_divider_ratio = 4.3;
constexpr float v_shunt_multiplier_ratio = 6;

//device-specific constants
constexpr int adc_max = 1023;
constexpr int dac_max = 255;
constexpr int v_max_mv = 5000;

//fet-cooling specific constants
constexpr float fet_power_max = 2; //(max continuous watts, depends on
heatsink)

//adjustable v_control_max. determines max current drawn from the source
(Rshunt = 1ohm, so Ishunt = Vshunt = Vcontrol)
constexpr int v_control_max_mv = 600;
//number of data points to take between 0 and v_control_max_mv
constexpr int n_steps = 60;
constexpr float fet_min_power = 0.1; //min power that triggers the stop of
data collection.

File log_file;
bool SDFileWriteLine(String text, String filename);
float analogRead_to_V(float analogRead_counts);
float analogWrite_to_V(float analogWrite_counts);
int collect_data_points(String &log_filename, int delay_ms, int
v_control_max_mv, int dac_increment); //returns an integer representing
the highest control voltage (mV) that produced power greater than
fet_min_power
void configure_pins();
void collect_data_two_step();
void setup() {

 configure_pins();
 Serial.begin(9600);
 while (!Serial) {
 ;
```

```
 }
 if (!SD.begin(CHIP_SELECT)) {
   Serial.println("Card failed, or not present");
   // don't do anything more:
   while (1) ;
 }

 int filename_idx = EEPROM.read(FILENAME_CNT_EEPROM_ADR); //get the
filename index
 String log_filename = "log_" + String(filename_idx) + ".csv"; //construct
the log filename
 Serial.println(log_filename);

 collect_data_two_step(log_filename);

 EEPROM.update(FILENAME_CNT_EEPROM_ADR, filename_idx+1); //update the
filename index for next run
}
int collect_data_points(String &log_filename, int delay_ms, int
v_control_max_analog, int dac_increment){
 SDFileWriteLine("VSource (V), VControl (V), VShunt (V), FetPower (W),
FetAvgPower (W)", log_filename); //write the log file's csv headers
  int fet_avg_power_loop_index = 0; //keep track of loop index (1 index)
to calculate avg power.
 float fet_power_total = 0; //running power tally for calculating avg
power.
 Serial.println("v_control_max_analog: " + String (v_control_max_analog));
   Serial.println("dac_increment: " + String (dac_increment));
 int fet_min_power_cnt = 0;
 for (int v_control_output = 0; v_control_output < v_control_max_analog;
v_control_output+=dac_increment)
 {
   fet_avg_power_loop_index++;
   float fet_power_predicted =
pow(analogWrite_to_V(v_control_output/v_control_divider_ratio), 2);
//predict fet power based on Rshunt = 1ohm and the control signal voltage
   fet_power_total += fet_power_predicted; //add to the total power...
   float fet_avg_power_predicted =
fet_power_total/fet_avg_power_loop_index; //to calculate avg power.

   Serial.println("Fet avg power predicted (W): " +
String(fet_avg_power_predicted));
   if (fet_avg_power_predicted>fet_power_max){
     Serial.println("Max avg. power would be exceeded, exiting current
test.");
     SDFileWriteLine("Max avg. power would be exceeded, exiting current
test.", log_filename);
```

```
      break;
    }

    analogWrite(3, v_control_output); //set the control output...
    delay(delay_ms); //and wait for the circuit response.

    int v_shunt_analog = analogRead(A0);
    int v_source_analog = analogRead(A1);
    float v_control =
analogWrite_to_V(v_control_output/v_control_divider_ratio);
    float v_shunt =
analogRead_to_V(v_shunt_analog/(float)v_shunt_multiplier_ratio);
    float v_source =
analogRead_to_V(v_source_analog*v_source_divider_ratio);
    float fet_power = (v_source-v_shunt)*(v_shunt);

    fet_power_total -= fet_power_predicted; //subtract the predicted
power...
    fet_power_total += fet_power; //add in the actual power to keep avg
accurate.

    float fet_avg_power = fet_power_total/fet_avg_power_loop_index; //to
calculate avg power.
    Serial.println("Fet avg power actual (W): " + String(fet_avg_power));
    Serial.println(String("V control (analogWrite): ") +
String(v_control_output));
    Serial.println(String("V control (V): ") + String(v_control, 3));
    Serial.println(String("V shunt (V): ") + String(v_shunt, 3));
    Serial.println(String("V source (V): ") + String(v_source, 3));
    Serial.println(String("fet power (W): ") + String(fet_power, 3));

    String csv_data = String(v_source,3) + "," +  String(v_control,3) + ","
+ String(v_shunt,3) + "," + String(fet_power,3) + "," +
String(fet_avg_power);
    SDFileWriteLine(csv_data, log_filename);

    if(fet_power < fet_min_power && fet_avg_power > fet_power){

      fet_min_power_cnt++;
      Serial.println("Minimum power reached..." + String(fet_min_power_cnt)
+ String("/3"));
      if(fet_min_power_cnt >= 3){
      Serial.println("Minimum power reached. Exiting.");
      SDFileWriteLine("Minimum power reached. Exiting.", log_filename);
      return v_control_output;
      }
    }
```

```
   Serial.println();
 }
}
void configure_pins(){
 pinMode(A0, INPUT);
 pinMode(A1, INPUT);
 pinMode(CHIP_SELECT, OUTPUT);
 pinMode(4, OUTPUT); //LED output process finished signal
}
bool SDFileWriteLine(String text, String filename)
{
 log_file = SD.open((filename).c_str(), FILE_WRITE);
 if (log_file) {
   log_file.println(text);
   log_file.close();
   //success
   return true;
 } else {
   //failed to open file
   return false;
 }
}
float analogRead_to_V(float analogRead_counts){
 return (float)analogRead_counts/adc_max*(float)v_max_mv / 1000.0F;
}
float analogWrite_to_V(float analogWrite_counts){
 return (float)analogWrite_counts/(float)dac_max*(float)v_max_mv /
1000.0F;
}
void collect_data_two_step(String &log_filename){
 //set parameters driven by v_control and n_steps
 static constexpr int v_control_max_analog_initial =
((float)(v_control_max_mv * v_control_divider_ratio)/(float)v_max_mv) *
dac_max;
 static constexpr int dac_increment_initial =
(float)(v_control_max_analog_initial + (n_steps - 1)) / (float)n_steps;

 // COLLECT DATA - FIRST PASS (Use default range)
 int v_control_max_analog_dynamic = collect_data_points(log_filename, 100,
v_control_max_analog_initial, dac_increment_initial); //vary the control
signal and collect data to Serial and SD
 int dac_increment_dynamic = (float)(v_control_max_analog_dynamic +
(n_steps - 1)) / (float)n_steps;
  //COLLECT DATA - SECOND PASS (Change range to fit DUT characteristic)
 collect_data_points(log_filename, 100, v_control_max_analog_dynamic,
dac_increment_dynamic); //vary the control signal and collect data to
Serial and SD. Use the newly determined dynamic maximum.
```

```
 digitalWrite(3, LOW); //shut down the control circuit
  log_file.flush(); //save the SD card

 Serial.print(log_filename);
 Serial.println(" saved.");
}
void loop() {
 //blink an LED to signal data collection finished
 digitalWrite(4, HIGH);
 delay(500);
 digitalWrite(4, LOW);
 delay(500);
}
```

Appendix C - Bill of Materials

Table 1C - Bill of Materials

Count	Name	Value	Description	Part ID	Manufacturer	Unit Cost ($)
7	0.125 W Resistor	1kΩ, 3.3kΩ, (2x) 20kΩ, (3x) 100kΩ	TH Axial Resistor	Generic	/	0.01
1	10 W Resistor	1Ω	TH Axial Power Resistor	Generic	/	0.5
1	Ceramic Capacitor	1 uF	Ceramic Capacior	Generic	/	0.01
1	N-E-MOSFET	/	N-E-MOSFET	PSMN4R3-30PL	Nexperia	1.20
1	ATMega328 Nano Development Board	/	Development Board	ATMega328 Dev. Board	Arduino	7.0
1	LM358	/	Dual op amp	LM358B	Texas Instruments	0.5
1	TO-220 Heatsink	15*10*5 mm^3 bulk	Generic TO-220 Heatsink	Generic	/	1.0
1	Perfboard	50*70 mm^2	Two-sided perfboard	Generic	/	0.5
-	-	-	-	-	TOTAL:	10.78

Appendix D - Analysis of Senior Project Design

Summary of Functional Requirements:
Our project aims to develop an affordable and versatile device for testing and analyzing solar panels, batteries, and other voltage sources. The primary objective is to create a portable, cost-effective, and space-efficient device that can be used in various scenarios, including the evaluation of remote microgrids and specialized systems. The device will enable users to gather crucial information about the voltage-current relationship, voltage-power relationship, and other power characteristics of each Device Under Test (DUT) across a range of load currents.

One key aspect of the device is its configurability, allowing users to easily modify device parameters and components to accommodate different use cases. This includes supporting lower or higher power sources, adapting to sources with different characteristic curves, and accommodating a wide input source voltage range. By providing users with digestible and valuable data, the device will facilitate the characterization and design of diverse energy systems that utilize these energy sources.

Primary Constraints
Limitations regarding system ability to measure low-power sources due to DAC minimum step. As we can see from the data, there are certain gaps in the measurements with respect to source voltage. The gaps in the data are caused by the limited resolution of the DAC which drives the electronic load. The DAC is only capable of 4.54mV increments to the control circuitry, which in the small and medium panels led to gaps in the I/V, P/V, and general data plots. This is due to the fact that the data curves of the smaller sources fall into a smaller range of currents, which we were unable to measure using our relatively low resolution electronic load system. Using a DAC with a better resolution, we would be able to drive the electronic load with a narrower current increment, and therefore collect data from the sources in narrower increments, and eliminate the gaps in the data. In addition to increasing the DAC resolution, we would also have to increase the ADC resolution, because as discussed earlier, the ADC resolution should be better or equal to the DAC resolution due to its role in the control circuitry on the output side of the electronic load. These problems could be controlled by improving the minimum step size to increase the accuracy as well as varying the control step to collect evenly spaced data w.r.t. source voltages.

Economic
The price of the materials for one manufactured unit is $10.78. The unit requires soldering and programming of the microcontroller, which should take less than an hour. Therefore, the device can be produced for under $40 per unit.

If Manufactured on a Commercial Basis

The device manufacturing time on a perfboard is low due to the low component count. However, a PCB would make the unit more compact and easy to transport. Additionally, the device manufacturing time can be reduced further through the use of third-party SMD assembly services for the placing and soldering of components. Each board will need to have its microcontroller programmed, which will add logistic complexity.

Environmental

The environmental implications of this device are positive as it helps to improve the efficiency of energy transfer between renewable energy sources and their desired load. The manufacturing of the circuit is relatively inexpensive resource wise with the most difficult component being the solar panels due to their cost and energy storage requirements. An improvement to this design would be altering the PCB to improve reliability, portability, and reduce the board footprint. This however would increase the price of production and would require additional protective circuitry if implemented at a larger scale.

Manufacturability

With the current size of the project there is little to no problem with manufacturing. All of the components used are mass produced by many companies with low costs and reasonable shipping times. If the project was altered to handle high power sources there would be additional components required with higher maxes and tighter tolerances which would increase price and the difficulty of manufacturing.

Sustainability

Overall the device is very sustainable and was designed to handle clean energy sources that help promote environmental conservation and the use of green energy. A potential problem with the sustainability of the project is the use of solar panels which takes on their potential drawbacks which include a high start up cost and requires lots of energy storage components on a larger scale. The project improves the sustainable use of resources as it was designed for clean energy sources and is portable and capable of functioning outdoors in various weather conditions. A possible improvement to this design would be altering the PCB to improve reliability, portability, and reduce the board footprint. A drawback to these improvements would be an increase in cost as other PCB boards or a custom one that is smaller and more efficient would directly increase the price of production

Ethical

The primary focus of the design is to provide efficient control of the key variables important in the control of power sources therefore there are little to no ethical precautions that need to be considered. This project is designed to improve the implementation of clean energy and help protect the environment while fulfilling people's needs.

Health and Safety

This device was created and tested for a wide range of power sources that are commonly used in everyday items however the components are not suitable for high power electronics therefore the design did not require additional safety measures. Due to the power requirements of the system there will not be any voltages or currents that are potentially dangerous however if this design was scaled up for high power units there would need to be additional safety improvements needed.

Social and Political

The stakeholders of this project include those invested in power and clean energy. As a result companies who push for the conversion to renewable energy will benefit the most while those invested in fossil fuels may be negatively affected. Politically those in favor of clean energy will likely invest and benefit the most from this project which could create pay inequalities for those reliant on the fossil fuel industry likely leading to some push back. Those who are pushing for clean energy tend to live in higher income areas which could separate the gap between rich and poor as well as induce job loss in the non-renewable resource industry further in the future.

Developmental

Given the ability of the device to characterize and empower the use of clean energy sources, the device will improve the development of clean energy sources. The device's ability to accurately measure and analyze the performance of clean energy sources, such as solar panels and batteries, allows for better understanding and optimization of their capabilities. This knowledge can facilitate improvements in energy conversion efficiency, storage capacity, and overall system design.

Furthermore, the device's portability and configurability make it suitable for various use cases, including remote microgrids and specialized systems. This versatility enables the testing and characterization of clean energy sources in diverse settings, providing valuable data for research and development efforts.